IOP Conf. Series: Materials Science and Engineering **418** (2018) 012006 doi:10.1088/1757-899X/418/1/012006

Interpretation of the abnormal high-temperature flow behavior of Fe-Mn-Al duplex lightweight steel

Lixiong Xu[1, 2], Huibin Wu[1] and Yinli Chen[1]

[1] Collaborative Innovation Center of Steel Technology, University of Science and Technology Beijing, Beijing 100083, China

[2] Corresponding author: E-mail: lixiongxu@163.com

Abstract. The hot deformation behaviors of two Fe-Mn-Al lightweight steels were investigated by hot compression tests on a Gleeble-3500 thermal simulation machine over a practical range of temperatures and strain rates. Optical microscope (OM) and electron backscattered diffraction (EBSD) were carried out to observe the microstructural mo rphologies of samples after hot deformation. Different from the single austenite steel, the hot compression tests of the duplex steel were actually carried out on an austenite/δ-ferrite duplex matrix with various phase compositions. At the commencement of deformation, strain was intensively distributed in δ-ferrite due to its higher stacking fault energy (SFE), and the dynamic softening behavior occurred earlier in δ-ferrite than in austenite during the whole hot deformation period. As a consequence, the prior dynamic recovery (DRV) in δ-ferrite caused the yield-like behavior, and the strain partitioning between δ-ferrite and austenite resulted to a visible serration on the flow curves. The dominant continuous dynamic recrystallization (CDRX) in δ-ferrite at high temperature caused a typical dynamic recovery characteristic, and the dominant discontinuous dynamic recrystallization (DDRX) in austenite at low temperature resulted in a typical dynamic recrystallization characteristic of the flow curves.

1. Introduction

Fe–Mn–Al lightweight steel has gained much attention due to the combination of its excellent mechanical properties, improved corrosion resistance, and low density [1]. With different Al/Mn equivalent ratios, this kind of steel could be distinguished into single ferrite, single austenite, and austenite–ferrite duplex structures [2]. The austenite-based duplex lightweight steel has been proved to have a nice combination of high strength and toughness, relying on the varying volume fraction and distribution of the hard secondary phase, δ-ferrite [3, 4].

During hot deformation, the ferrite phase, characterized by relatively high stacking fault energy (SFE) values, tends to soften through intense dynamic recovery (DRV) because of the easy cross-slip of dislocation [5]. This process might gradually evolve into continuous dynamic recrystallization (CDRX), also known as „extended" DRV, which is associated with the conversion of low angle boundaries (LABs) into high-angle boundaries (HABs) during straining [6, 7]. However, the austenite phase, in which cross-slip of dislocation is restricted due to the lower SFE, tends to be softened by discontinuous dynamic recrystallization (DDRX), associated with the formation of new grains through nucleation and growth after an insufficient DRV [8]. In addition, it was reported in duplex steels that the strain was mostly concentrated on the δ-ferrite phase at the commencement of deformation and austenite experienced the main strain subsequently [9]. Hence, the existence of δ-ferrite makes the hot deformation behavior more complicated in the austenite-based duplex steel, which is similar to the characteristic of Cr-Ni duplex stainless steel [10].

Characterizing the hot deformation behavior of steel is the theoretical basis of the thermal mechanical control processing (TMCP). Recent research on the hot deformation behavior of Fe-Mn-Al lightweight steel has mostly focused on the data analysis relying on the true stress-train curves [11-13]. Li et al. established a DRX kinetic model of an austenite-based duplex steel by flow stress and peak strain without considering the DRV and DRX in δ-ferrite, and concluded that the increasing deformation temperature or strain rate contributed to DRX in both the austenite and the δ-ferrite phase. However, it was contrary to the fact that the flow curves exhibited a greater dynamic softening at low temperatures [14]. Accordingly, the dissimilar plastic behaviors of ferrite and austenite as well as the varying phase composition make it difficult to clarify the hot deformation behavior of the duplex steel only according to the flow curves.

This study aimed at interpreting the hot deformation behavior of Fe-Mn-Al duplex lightweight steel by microstructural evolution of dynamically compressed specimens, coupled with the true stress-strain curves. For comparative purposes, the experimental hot compression tests of two Fe-Mn-Al lightweight steels, containing single austenite structure (austenite steel) and austenite/δ-ferrite duplex structure (duplex steel) respectively, were conducted on a Gleeble-3500 thermal simulation machine in the temperatures range of 800–1050 °C and strains rates range of 0.01–10 s^{-1}.

2. Materials and Methods

The materials used in the research consisted of two laboratory cast Fe-Mn-Al steels containing single austenite phase (designated "austenite steel"), austenite and δ-ferrite dual-phase structure (designated "duplex steel"). Ingots with weight of 25 Kg were prepared in a vacuum induction melting furnace. After homogenization at 1150 °C for 2 h, the ingots were forged into rectangular billets of 80 mm×80 mm×100 mm. The compositions of the two Fe-Mn-AL steels were measured by Sheffield Testing Laboratories and are listed in Table 1. The scanning electron microscopy (SEM) images and X-ray diffraction (XRD) analysis of the forged microstructure of the two steels are shown in Figure 1. It reveals that the austenite steel contains a single phase structure, with plenty of annealing twins distributing in the austenite matrix. The duplex steel consists of 82.6% austenite and 17.4% δ-ferrite, with the discontinuous δ-ferrite network distributing along the austenite grain boundaries. The densities of the austenite steel and duplex steel, measured by Sartorius BSA 2245 electronic analytical balance, are 7.19 $g \cdot cm^{-3}$ and 6.98 $g \cdot cm^{-3}$ respectively, with a reduction of 8.5% and 11.2% in comparison with pure iron.

Table 1. Chemical composition of the laboratory steels (wt%).

	C	Mn	Al	Fe
Austenite steel	0.05	24.0	4.0	Bal.
Duplex steel	0.05	26.0	6.0	Bal.

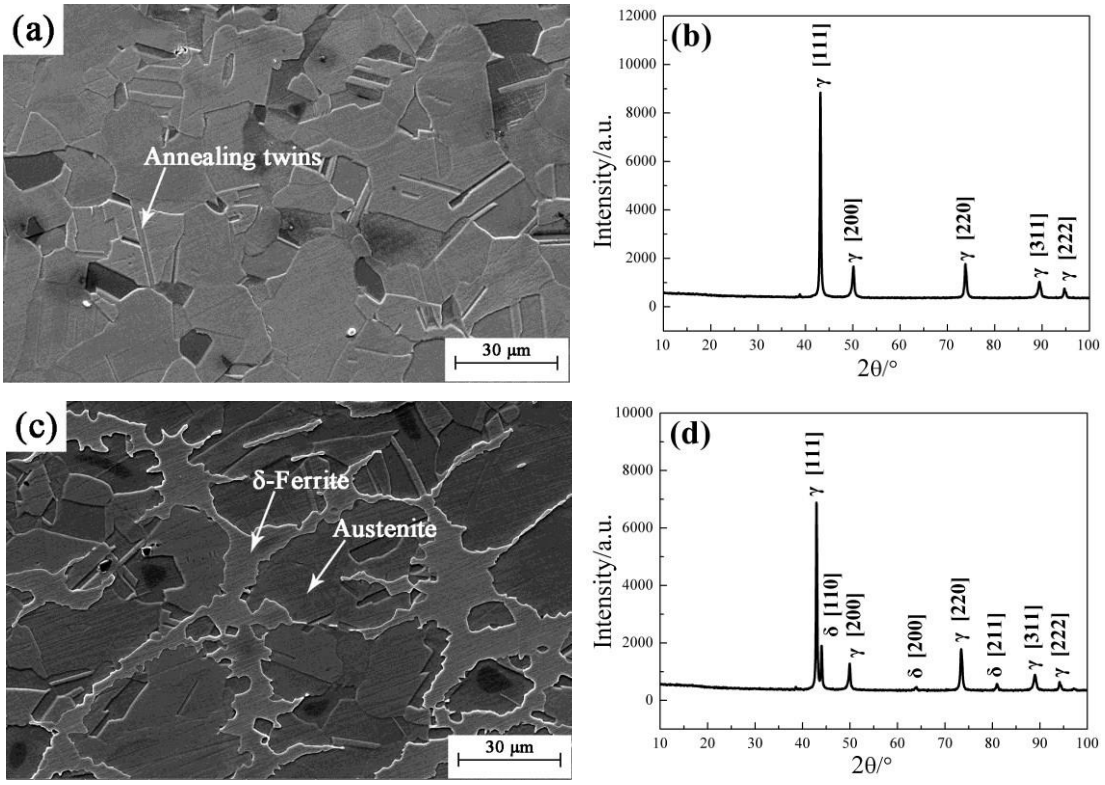

Figure 1. SEM image and XRD pattern of the forged microstructure of (a) (b) austenite steel and (c) (d) duplex steel (δ: δ-ferrite; γ: austenite).

Samples of Φ10 mm ×15 mm were cut off from the forged billets for unidirectional axisymmetrical compression tests on a Gleeble-3500 thermo-simulation machine. The uniform simulation scheme of the two steels is shown in Figure 2. The specimens were initially heated to 1100 °C at a rate of 5 °C/s, soaked for 2 min to completely homogenize the temperature field, and then cooled down to the predetermined deformation temperature at a rate of 10 °C/s. After holding isothermally for 20 s to maintain a uniform temperature distribution throughout the cylinder, the specimens were compressed at temperatures ranging from 800 to 1050 °C and strain rates ranging from 0.01 to 10 s^{-1}, with a true strain of 0.9. Finally, all the specimens were cooled to the ambient temperature at a cooling rate of 30 °C/s to preserve the high temperature structure.

After the compression tests, the microstructure of central areas of the specimens were analyzed by optical microscope (OM), and electron backscattered diffraction (EBSD) using a field-emission scanning electron microscope (FESEM, Zeiss Ultra 55) at an acceleration voltage of 15 kV with a step size of 0.25 μm. The specimens prepared for EBSD were sectioned at mid-plane perpendicularly to the compression direction and electro-polished in an electrolyte solution of 20/80 (v/v) perchloric acid and ethanol for 15 s, at a voltage of 15 V and current of 1.5 A.

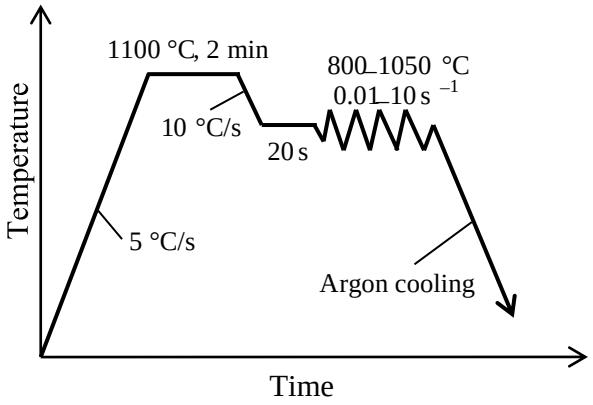

Figure 2. Thermo-mechanical simulation scheme for both austenite steel and duplex steel.

3. Results

3.1. Mechanical Response

Due to the combined effects of work hardening (WH), DRV, and DRX, most of the flow stress curves can be classified into three types: work-hardening, showing an increasing stress with the increasing strain; dynamic recovery, exhibiting a saturation stress within the whole strain range; dynamic recrystallization, characterized by an observed peak stress followed by an decreasing stress prior to steady stress [15].

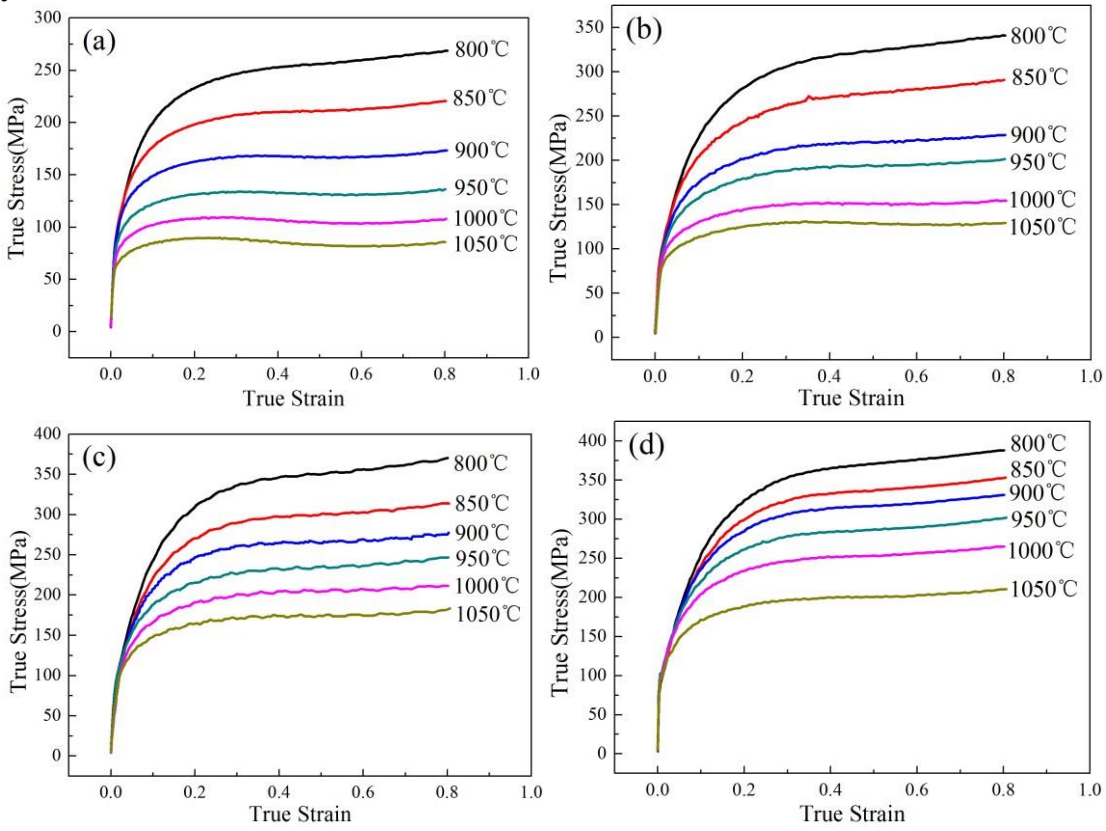

Figure 3. True stress-strain curves of austenite steel deformed at strain rates of (a) 0.01 s^{-1}, (b) 0.1 s^{-1}, (c) 1 s^{-1} and (d) 10 s^{-1}.

The true stress-strain curves of the austenite steel exhibit same characteristics common to some other studies [16, 17], as shown in Figure 3. The flow stress decreases with the increasing deformation temperature and decreasing strain rate. When strain rate is 0.01 s^{-1} and deformation temperature is greater than 950 °C, the flow stress curves exhibit typical dynamic recrystallization behavior with a single peak stress followed by a gradual fall toward a steady stress, which was caused by an intense dynamic softening effect during hot deformation. With the decrease in deformation temperature and the increase in strain rate, the dynamic softening was inhibited due to the low average kinetic energy of atoms and short duration of deformation, and accordingly, storage energies during deformation increased and more defects such as dislocation and vacancy were reserved. Therefore, aside from the several dynamic recrystallization curves in Figure 3(a), other curves exhibit the typical work-hardening characteristic.

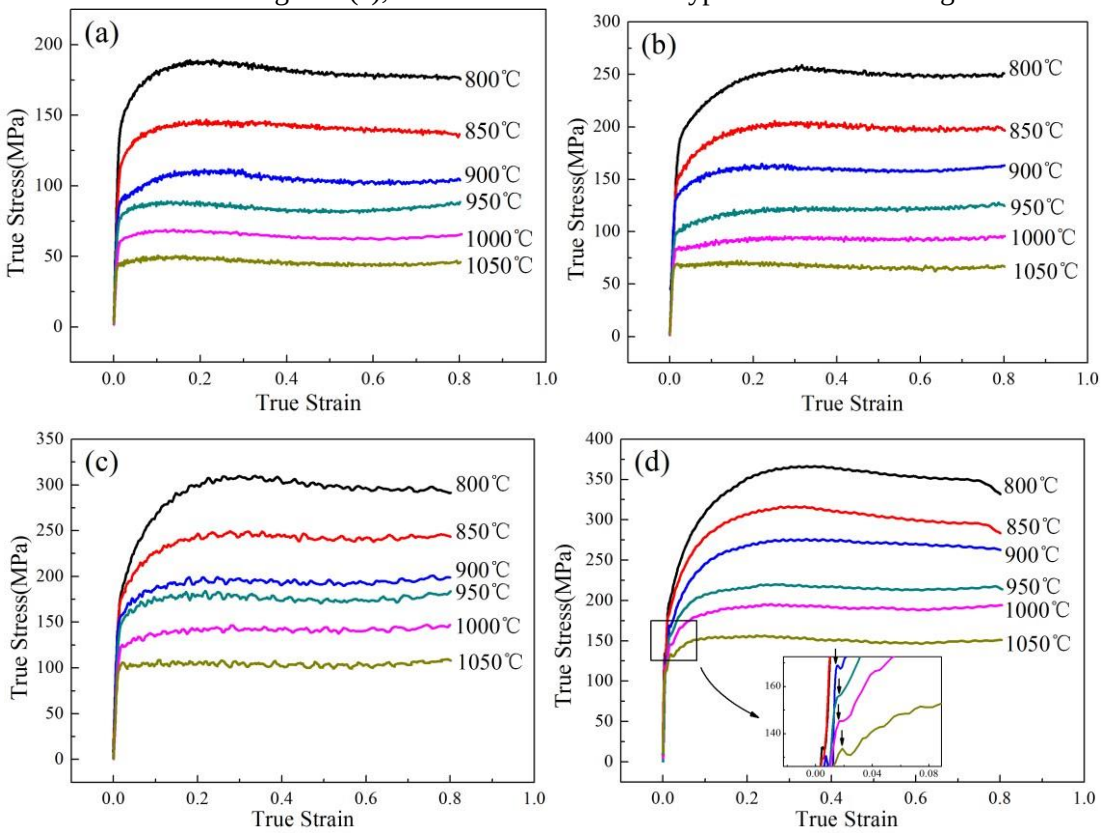

Figure 4. True stress-strain curves of duplex steel deformed at strain rates of (a) 0.01 s^{-1}, (b) 0.1 s^{-1}, (c) 1 s^{-1}, (d) 10 s^{-1}.

The true stress-strain curves of the duplex steel show several abnormal characteristics compared to the austenite steel, as shown in Figure 4. In the first place, the stress level in duplex steel is obviously lower than that in austenite steel under the uniform deformation conditions. Secondly, at a temperature lower than 900 °C, the flow curves exhibit initial WH followed by a single broad stress peak and a slight decline before steady stage, indicating the occurrence of DRX. As the temperature increases, the initial WH becomes inconspicuous and the flow curves display a long steady stage after reaching a peak value, showing a typical dynamic recovery characteristic. That is an abnormal dynamic softening behavior versus to the common flow curves [18, 19]. Furthermore, at high deformation temperature and high strain rate, the yielding plateaus with pronounced upper and lower yield points are found in the magnified area in Figure 4(d), which is an indication of yield-like behavior similar to the yield point elongation-like effect in a 2205 duplex stainless steel [20]. In addition, the flow curves of duplex steel exhibit a more visible serration compared to austenite steel under the whole deformation conditions.

The dependences of phase volume fractions on the deformation temperature of the austenite steel and duplex steel, calculated by the Thermal-Calc software, are shown in Figure 5. It reveals that the hot

compression processes of the austenite steel were carried out on a single austenite phase within the whole temperature range, while the duplex steel was actually compressed at a duplex matrix with a varying phase composition. As the deformation temperature increases from 800 °C to 1050 °C, the volume fraction of austenite decreases from 77.3% to 45.6%, and that of δ-ferrite increases from 22.7% to 54.4%. Accordingly, the distinct high-temperature flow behavior of the duplex steel compared to the austenite steel may result from the great impact of δ-ferrite on the hot deformation behavior of austenite-based duplex steel.

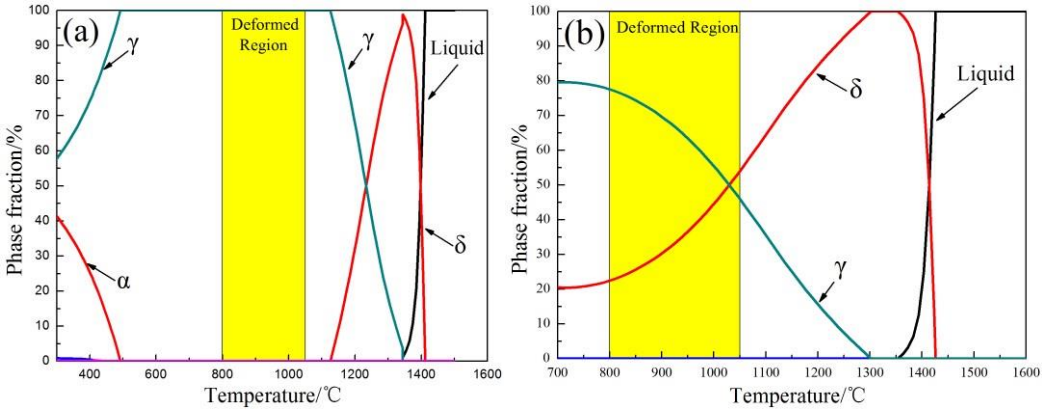

Figure 5. Dependence of phase volume fractions on temperature of the (a) austenite steel and (b) duplex steel (γ: austenite; δ: δ-ferrite; α: α-ferrite).

3.2. Microstructural response

The micrographs observed by OM of the austenite steel deformed at different temperatures and strain rates are shown in Figure 6, where RD and AD denote the radial direction and axial direction of the compressed cylinder specimens respectively. Comparing the microstructures deformed at strain rate of $0.01s^{-1}$, a mixed structure of initial deformed grains and fine DRX grains can be observed at 850 °C (Figure 6(a)), indicating the incomplete dynamic recrystallization of austenite. When the deformation temperature increases to 950 °C, many deformed grains are gradually replaced by the fine DRX grains (Figure 6(b)). As the temperature further increases to 1050 °C, a completed DRX microstructure is visible (Figure 6(c)), which indicates that the DRX degree notably increased with the increasing deformation temperature. This is because the dislocation motion and crystal slip became easy due to the higher average kinetic energy of atoms at a relatively high temperature [21]. Also, the high temperature enhanced the grain boundary migration mobility by increasing the diffusivity of elements, which facilitated the nucleation and growth of DRX grains [22].

When the strain rate increases to $10s^{-1}$, many banded grains (perpendicular to the compression direction) are observed in the whole temperature range (Figure 6(d)-(f)). The uneven microstructure and the decreasing DRX grains indicate that the dynamic recrystallization of austenite was heavily suppressed at high strain rate. The few DRX grains formed in presumably highly stressed locations close to the grain boundaries suggest a restoration mechanism of DDRX, which was extremely limited and mainly occurred though strain-induced boundary migration (SIBM) of the original austenitic boundaries [23]. Although high strain rate can enhance the nucleation of DRX, it is widely accepted that high strain rate can also retard the growth of DRX nuclei [24]. Thus, the DRX induced dynamic softening was slight and the work hardening dominated the flow curves at relatively high strain rate (Figure 3).

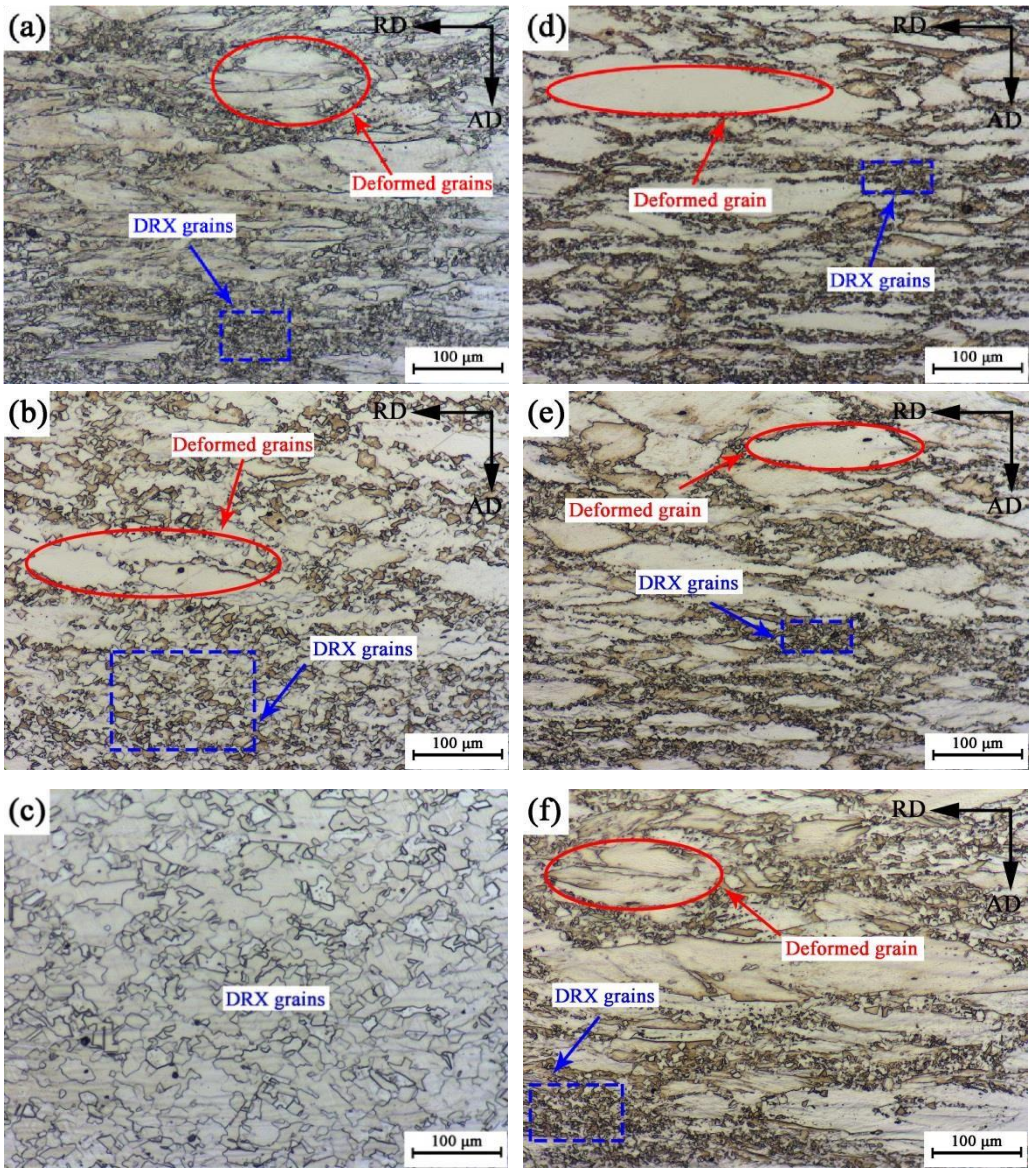

Figure 6. OM image of the microstructure of austenite steel deformed at (a) 0.01 s^{-1} and 850 °C, (b) 0.01 s^{-1} and 950 °C, (c) 0.01 s^{-1} and 1050 °C, (d) 10 s^{-1} and 850 °C, (e)10 s^{-1} and 950 °C and (f) 10 s^{-1} and 1050 °C.

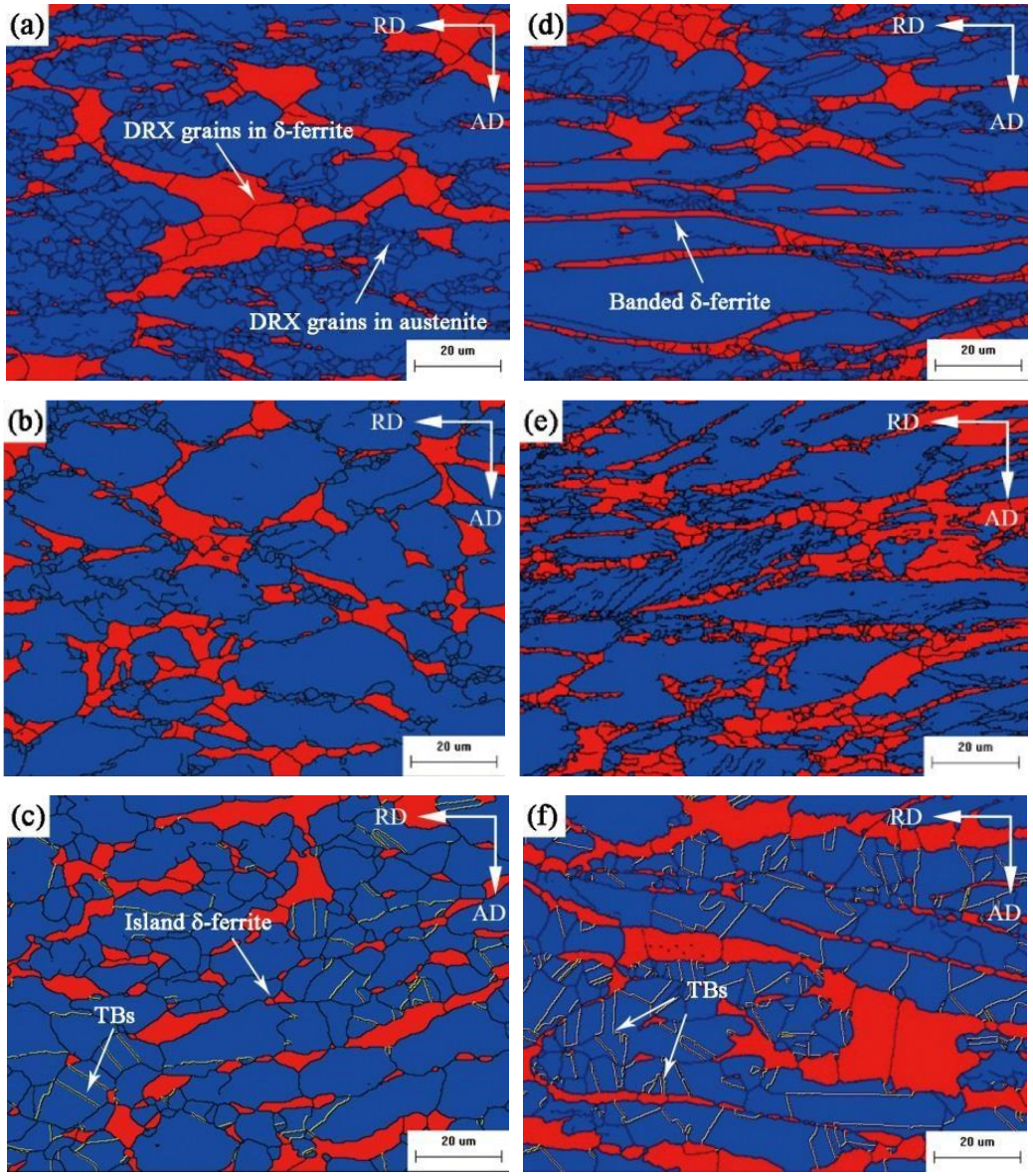

Figure 7. EBSD analysis (showing austenite in blue, δ-ferrite in red, HABs in black lines, and MTs in yellow lines) of the microstructure of duplex steel deformed at (a) 0.01 s^{-1} and 850 °C, (b) 0.01 s^{-1} and 950 °C, (c) 0.01 s^{-1} and 1050 °C, (d) 10 s^{-1} and 850 °C; (e) 10 $s^{-1}$and 950 °C, (f) 10 s^{-1} and 1050 °C.

Figure 7 shows the EBSD analysis of the microstructure of duplex steel deformed at different conditions. At strain rate of 0.01 s^{-1} and temperature of 850 °C, the equiaxed HABs inside the original δ-ferrite grains (Figure 7(a)) are an indication of CDRX, which was evolved from the LABs formed during the efficient DRV [25]. The partial tiny austenite grains associated with HABs and distributed in the austenite boundaries indicate a softening mechanism of DDRX resulting from SIBM. As the temperature increases to 950 °C, the number of DRX grains in austenite decreases obviously (Figure 7(b)), showing an abnormal microstructural response versus to the austenite steel. Meanwhile, δ-ferrite is distributed discretely in the austenite matrix, implying that the DRX process was suppressed in austenite while promoted in δ-ferrite. As the temperature further increases to 1050 °C, the abundant twin boundaries (TBs, marked as yellow lines in Figure 7 (c)) reveal that DDRX of austenite mainly occurred

through the formation of multiple twinning chains. The coarsening of few austenitic DRX grains at high temperature led to an uneven microstructure and separated δ-ferrite into island structures.

As the strain rate increases from 0.01 to 10 s^{-1}, the duration of deformation was shortened, so that the DRXs in both austenite and δ-ferrite were postponed, characterised by the fewer tiny DRX grains in austenite and smaller DRX grains in δ-ferrite which appear near original grain boundaries (Figure 7(d) and (e)). So the flow curves display an increasing stress level with the increasing strain rate, as shown in Figure 4. Meanwhile, the stronger strain hardening led to local accumulations of dislocation densities in the material and turned δ-ferrite into discontinuous bands which are perpendicular to the squeezing direction. As the temperature increases to 1050°C, the sufficient distortion energy stimulated the occurrence of a large number of TBs in the original austenite grains (Figure 7(f)), which indicates a main DDRX mechanism of multiple twinning similarly. Owing to the repressed softening behavior and the promoted WH behavior at the high strain rate, the δ-ferrite bands were preserved even at a high temperature.

4. Discussion

In general, the diffusion rate of elements in δ-ferrite is about an order of magnitude higher than that in austenite. Moreover, the dislocation movement in δ-ferrite is faster than that in austenite due to its higher SFE [26]. Therefore, the deformed zones in the duplex steel were mostly located in the vicinity of the interphase boundaries and almost always on the δ-ferrite side, which caused a focused distribution of deformation in δ-ferrite at the early stage of deformation. The higher SFE also resulted in a relative ease for dislocation to climb or cross-slip as an expression of the lower apparent activation energy of δ-ferrite [27]. As a consequence, the dynamic softening commenced with DRV in δ-ferrite which caused the yield-like behavior on the flow curves. The larger DRX grains in δ-ferrite than in austenite verified that the DRV and DRX occurred primarily in δ-ferrite during hot deformation (Figure 7(a)). As the deformation proceeded, strain was transferred from δ-ferrite to austenite, then the WH occurred in austenite, which increased the flow stress to a maximum. As the WH effect was balanced by the combined softening effect in δ-ferrite and austenite, the flow curves displayed a steady stress. In addition, the severely uneven distribution of strain in the duplex structure caused the visible serration on the flow curves, as shown in Figure 7.

Above all, the abnormal high-temperature flow behavior of duplex steel can be mainly interpreted by the interaction of strain partitioning and unsynchronized softening behavior in δ-ferrite and austenite at various deformation conditions. At high temperature (above 900 °C), the strain partition between δ-ferrite and austenite was enlarged and the strain levels partitioned into austenite were reduced due to the increasing volume fraction of δ-ferrite (Figure 5). Then the distortion energy was mostly eliminated by the efficient DRV in δ-ferrite at the commencement of plastic deformation, which decreased the dislocation density and reduced the subsequent driving force for dynamic softening in austenite. Hence, the WH caused mainly by dislocation tangles in austenite was weakened, and the dominant CDRX in δ-ferrite caused a typical dynamic recovery characteristic of the flow curves. As the strain levels in austenite were not high enough to convert the pre-existing austenite grain boundaries into general HABs capable of SIBM, the dominant DRX mechanism in austenite was converted from SIBM to multiple twining and the DRX extent in austenite was reduced (Figure 7 (c) and (f)). At low temperature (below 900 °C), the softening effect caused by DRV in δ-ferrite was restricted due to the decreasing δ-ferrite content (Figure 5) and the lower average kinetic energy of atoms. The rapid transfer of load from δ-ferrite to austenite enhanced the WH by the increasing dislocation density and facilitated the initiation of DDRX in austenite caused by SIBM. That resulted in the intense WH stage and a typical dynamic recrystallization characteristic of the flow curves. Meanwhile, the yield-like behavior was covered with the intense WH effect at the commencement of plastic deformation at low temperature (Figure 4).

At low strain rate (0.01 s^{-1}), more load was transferred from δ-ferrite to austenite due to the long duration of deformation. So the softening effect of DRV in δ-ferrite was not efficient enough to stimulate a conspicuous yield-like behavior at the early state of deformation, as shown in Figure 4. As the strain rate increased from 0.01 to 10 s^{-1}, the uneven strain partition between δ-ferrite and austenite was further

enlarged due to the reduced duration of deformation and the restricted strain levels partitioned into austenite. So both the yield-like behavior and the difference between the flow behavior at high- and low-temperatures became more conspicuous. Moreover, since it was difficult for dynamic softening in δ-ferrite and austenite to develop in a timely manner, the WH degree in the flow curves was intensified due to the quickly reproduced dislocations in austenite, as the strain rate increased.

5. Conclusions

(1) The hot deformation of the Fe-Mn-Al duplex steel was actually carried out at a duplex matrix with a varying phase composition. As the deformation temperature increases from 800 °C to 1050 °C, the volume fraction of austenite decreases from 77.3% to 45.6%, and that of δ-ferrite increases from 22.7% to 54.4%.

(2) Due to the higher SFE and the higher diffusion rate of elements in δ-ferrite, strain was intensively distributed in δ-ferrite at the early stage of deformation, and the dynamic softening behavior occurred earlier in δ-ferrite than in austenite during hot deformation. As a consequence, the prior DRV in δ-ferrite caused the yield-like behavior, and the severely uneven distribution of strain in the duplex structure resulted to the visible serration on the flow curves.

(3) At high temperature (above 900 °C), the strain partition between δ-ferrite and austenite was enlarged due to the increasing volume fraction of δ-ferrite, the dominant CDRX in δ-ferrite caused a typical dynamic recovery characteristic of the flow curves. At low temperature (below 900 °C), the DRV in δ-ferrite was restricted due to the decreasing δ-ferrite content and the lower average kinetic energy of atoms. The dominant DDRX in austenite resulted in a typical dynamic recrystallization characteristic of the flow curves. As the strain rate increased from 0.01 to 10 s^{-1}, the uneven strain partition between δ-ferrite and austenite was further enlarged, so both the yield-like behavior and the difference between the flow behavior at high- and low- temperatures became more conspicuous.

Acknowledgments

This research was financially supported by the National Key Research and Development Plan of China (No. 2017YFB0305000).

References

[1] Seo C H, Kwon K H, Choi K, Kim K H, Kwak J H, Lee S and Kim N J 2012 *Scr. Mater.* **66** 519-22
[2] Yang Q, Wang J F and Cong Y 2015 *Baosteel Technol* **3** 1-10
[3] Yang F Q, Song R B, Sun Ting, Zhang L F, Zhao C and Liao B X 2014 *Acta Metall. Sin.***50** 897-904
[4] Zhang L F, Song R B, Zhao C and Yang F Q 2015 *Mater. Sci. Eng.* A **640** 225-34
[5] Li H B, Jiao W C, Feng H, Li X X, Jiang Z H, Li G P, Wang L X, Fan G W and Han P D 2016 Metals **6** 223-39
[6] Haghdadi N, Cizek P, Beladi H and Hodgson P D 2017 *Acta Mater.* **126** 44-57
[7] Samantaray D, Mandal S, Jayalakshmi M, Athreya C N, Bhaduri A K and Sarma V S 2014 *Mater. Sci. Eng.* A **598** 368-75
[8] Van Do V N, Lee C H and Chang K H 2015 *Mater. Design* **65** 1161-71
[9] Fan G W, Liu J, Han P D and Qiao G J 2009 *Mater. Sci. Eng.* A **515** 108-12
[10] Haghdadi N, Martin D and Hodgson P 2016 *Mater. Design* **106** 420-427
[11] Choi J H 1997 Korean J. Met. Mater. **35** 3-7
[12] Yang F Q, Song R B, Zhang L F and Zhao C 2014 Procedia Engineering **81** 456-61
[13] Xu T C, Peng X D, Qin J, Chen Y F, Yang Y and Wei G B 2015 *J. Alloy Compd.* **639** 79-88
[14] Li Y P, Song R B, Wen E D and Yang F Q 2016 *Acta Metall. Sin. (Engl. Lett.)* **29** 441-49
[15] Xie B, Cai Q W, Wei Y, Xu L X and Ning Z 2016 *J. Mater. Eng. Perform.* **25** 5127-5137

[16] Babu K A and Mandal S 2017 *Mater. Sci. Eng.* A **703** 187-95
[17] Mehtonen S V, Karjalainen L P and Porter D A 2014 *Mater. Sci. Eng.* A **607** 44-52
[18] Lin Y C, Nong F Q, Chen X M, Chen D D and Chen M S 2017 *Vacuum* **137** 104-14
[19] Xie B S, Cai Q W, Yu W, Xu L X and Ning Z 2017 *Acta Metall. Sin. (Engl. Lett.)* **30** 250-60
[20] Chen L, Wang L M, Du X J and Liu X 2010 *Acta Metall. Sin.* **35** 52-56
[21] Wen D X, Lin Y C, Li H B, Chen X M, Deng J and Li L T 2014 *Mater. Sci. Eng.* A **591** 183-92
[22] Momeni A, Ebrahimi G R and Faridi H R 2015 *Mater. Sci. Eng.* A **626** 1-8
[23] Haghdadi N, Cizek P, Beladi H and Hodgson P D 2017 *Philos. Mag.* **97** 1209-37
[24] Roodposhti P S, Sarkar A and Murty K L 2015 *Mater. Sci. Eng.* A **626** 195-202
[25] Castan C, Montheillet F and Perlade A 2013 *Scr. Mater.* **68** 360-64
[26] Li J, Gong C, Chen L, Zuo H and Liu Y 2014 *Acta Metall. Sin.* **50** 1063-70
[27] Lin G Y, Zhang Z F, Zhang H, Peng D S and Zhou J 2008 *Acta Metall. Sin. (Engl. Lett.)* **21** 109-15